

Resonant magnetic quantum tunneling through thermally activated states

Fernando Luis, Juan Bartolomé, and Julio F. Fernández*

Instituto de Ciencia de Materiales de Aragón, Consejo Superior de Investigaciones Científicas and Universidad de Zaragoza, 50009-Zaragoza, Spain

(Received 23 May 1997)

We present a theory of resonant quantum tunneling of large spins through thermally activated states. It gives numerical results that are in good agreement with data from recent magnetic quantum tunneling experiments in Mn acetate. We show that neither dipolar fields nor crystal-field perturbations, acting separately, can account for the resonances observed. However, we find that these two perturbations acting *jointly* produce a highly nonlinear effect that enhances tunneling rates up to their observed values. Resonant tunneling through low-lying energy-state pairs is blocked. We show that the tunneling frequency ω_T and the lifetime τ_0 of the thermally populated pairs of states through which tunneling proceeds fulfills $\omega_T\tau_0 \gg 1$. A superposition of these two states becomes incoherent approximately in time $1/\omega_T$. Using the master equation that follows, and spin-phonon-induced transition rates that we calculate, we obtain relaxation rates and magnetization hysteresis curves that agree reasonably well with experiment.

[S0163-1829(98)00202-1]

I. INTRODUCTION

Magnetic quantum tunneling (MQT) of large spins has aroused much interest recently. A good portion of the interest stems from the expectation that MQT will contribute to our understanding of the role that decoherence effects, brought about by dissipation, play in the transition from quantum to classical physics.^{1,2} For some years, MQT has been searched for in single-domain ferromagnetic particles with large spins that rotate as a whole and with large anisotropy barriers between states of opposite spin orientations.³ Such large spins fluctuate fairly rapidly at high temperature, giving rise to "superparamagnetism."⁴ Classically, the relaxation rate Γ would vanish with the temperature T , but it has been predicted that MQT of single-domain particles is not negligible,⁵ and that it can be observed experimentally in highly anisotropic magnetic materials at liquid-helium temperatures.⁶

Experiments with these systems did not lead to definitive results.^{7,8} Particles come in different sizes, and their easy magnetization axes are randomly oriented. This leads to a broad distribution of relaxation times that obscures interpretation.⁹⁻¹¹ More recently, molecular crystals that are ideally suited for magnetic quantum tunneling experiments have been synthesized. Mn acetate is one of them. Each molecule has eight Mn^{3+} and four Mn^{4+} ions, with a total spin $S=10$ (S is given in units of \hbar throughout) and a large single-axis anisotropy that favors $\pm S$ spin alignment.¹² The anisotropy axis is oriented along the c crystalline axis (let it be the z axis). Magnetic interactions between different molecules are very weak in these crystals.¹² The fact that all molecules are identical has led to the experimental determination of a unique relaxation time.¹³

Striking jumps in magnetization hysteresis curves of Mn acetate crystals, for temperatures in the range $2 \text{ K} \leq T \leq 3 \text{ K}$, have very recently been reported.¹⁴⁻¹⁶ The magnetization jumps at values of an applied field along the anisotropy axis, given by $H_z^0 \approx nH_1$, where $n=0, \pm 1, \pm 2, \dots$ and

$H_1 \approx 0.5 \text{ T}$. At these temperatures, thermal population of excited states is far from negligible, since $U/(k_B S) \approx 6 \text{ K}$ in Mn acetate, where U is the energy barrier between states of opposite spin orientations, k_B is Boltzmann's constant, and $(U/S)(2-1/S)$ is the lowest excitation energy. Furthermore, frequency-dependent magnetic susceptibility experiments performed with a small ac field applied parallel to the dc field, at temperatures in the range $4 \text{ K} \leq T \leq 6 \text{ K}$, also give relaxation times that have sharp minima at the same field values, $H_z^0 \approx nH_1$. In addition, Γ is observed to decrease over several orders of magnitude as T decreases following Arrhenius' law for all values of H .^{15,17}

These experimental results clearly suggest (1) that unassisted MQT takes place when there is resonance¹⁸ between states of opposite spin orientation at field values $H_z^0 \approx nH_1$ (for $n=0, \pm 1, \pm 2, \dots$), and (2) that the resonant MQT observed takes place through thermally activated states. *Thermally activated resonant tunneling* of large spins had not, to our knowledge, been foreseen.¹⁹ Incidentally, thermally activated tunneling must also play a significant role in all experiments in Ref. 7, where $k_B T \sim U/S$ is fulfilled. (Experimental conditions reported in Ref. 8, on the other hand, do fulfil $k_B T \ll U/S$, and are, for that reason, beyond the scope of this paper. Experiments in which $k_B T \ll U/S$ is satisfied have also been performed on Mn acetate,²⁰ and Politi *et al.*²¹ have obtained the corresponding nonresonant rates for phonon-assisted tunneling from the lowest-lying metastable state.)

Important observations on Mn_{12} acetate remain unexplained. Experiments performed at $T \approx U/k_B S$ (Refs. 15,17) show that resonant MQT takes place mostly through $m=4, -4$ states when no magnetic field is applied. Why not through some more easily accessible lower energy states? Effects that are related are observed in the magnetization hysteresis curves that have recently been reported.^{14,16} No quantitative account has been given.²² We aim to fill this gap.

In this paper we establish how two leading spin interactions in Mn_{12} acetate, acting jointly, overcome effects that

inhibit tunneling. This is the seed of the desired explanation. Knowledge of the nature of these interactions enables us to estimate the values of the tunneling frequency ω_T . It turns out that $1/\omega_T$ is much smaller than spin-phonon interaction-induced lifetimes for all tunneling channels that are not blocked in Mn_{12} acetate. Tunneling through such long-lived states is shown to take place incoherently. Using the standard master equation that is then applicable, we obtain numerical results that agree well with experiments.

The plan of the paper is as follows. In Sec. II we describe the various terms that make up the spin Hamiltonian for Mn_{12} acetate. We discuss how dipolar magnetic fields along the anisotropy axis and hyperfine interactions inhibit spin tunneling through low-lying energy states. We find that only the combined action of transverse dipolar fields and quartic spin perturbations can account for the resonant MQT effects observed experimentally in Mn_{12} acetate. In Sec. III, we assume that spin-phonon interactions are the dominant nonstationary perturbations that lead to thermal equilibrium. A thermally excited-state pair $|E_l\rangle, |E_{l+1}\rangle$ decoheres in time given by $\hbar/\Delta E_{l+1,l}$ approximately, where $\Delta E_{l+1,l} = E_{l+1} - E_l$. We explain how incoherent superpositions of state pairs that are not tunnel blocked (and last for times τ_0 that are much longer than $\hbar/\Delta E_l$ in Mn acetate) give rise to the observed resonances in $\Gamma(H)$. More quantitatively, we show that the density matrix is approximately diagonal, while tunneling takes place, for systems in which τ_0 is much larger than $\hbar/\Delta E_{l+1,l}$. The standard master equation is then applicable. We obtain $\Gamma(H)$ and magnetization $m(H)$ hysteresis curves numerically for various temperatures. Agreement with experimental results^{14–17} is satisfactory.

II. RESONANT TUNNELING CONDITIONS

In this section, we discuss how easily MQT through low-lying energy states becomes blocked. The criterion that must be met for resonant tunneling to ensue enables us to establish the role that various interactions play in resonant MQT in Mn acetate crystals. The main purpose of this section is to show that crystal-field perturbations acting *jointly* with spatially random magnetic-field effects (that arise from hyperfine interactions) give highly nonlinear effects that can account for the observed resonant MQT in Mn acetate.

A. Hamiltonian

Consider,

$$\mathcal{H} = \mathcal{H}_0 + \mathcal{H}'_1 + \mathcal{H}'_2, \quad (1)$$

where

$$\mathcal{H}_0 = -DS_z^2 - g\mu_B H_z^0 S_z, \quad (2)$$

D is an anisotropy constant, H_z^0 is the z component of the applied field, S_z is a z component spin operator, $g = 1.9$,¹² is the gyromagnetic ratio, μ_B is the Bohr magneton, and \mathcal{H}'_1 and \mathcal{H}'_2 are stationary perturbations. This spin Hamiltonian has been proposed for Mn acetate crystals.¹³ There are 12 Mn ions in each of the identical Mn acetate molecules that make up the crystal. All Mn_{12} complexes have 8 $\text{Mn}^{3+}S = 2$ and 4 $\text{Mn}^{4+}S = 3/2$ ions. There is experimental evi-

dence that all Mn complexes have effective spins, with approximately constant $S = 10$ values, that are well isolated from each other, and that there is a single axis anisotropy along the c crystal axis (that we shall refer to as the z axis).¹³

We lump all terms that are diagonal in S_z in \mathcal{H}'_1 and put all off-diagonal ones into \mathcal{H}'_2 . Three kinds of interactions are taken into account. There are dipolar magnetic fields, \mathbf{H}_d , that vary (approximately) randomly over space. Hyperfine interactions cannot be neglected. Their effect on a Mn acetate spin is comparable to that of a magnetic field that is several times larger than \mathbf{H}_d .²³ We show in Appendix B that, at least for $H_z^0 \simeq nH_1$ and n even, the effect of hyperfine interactions on resonant MQT in Mn acetate is well approximated by a magnetic field that varies spatially randomly. Accordingly, we lump hyperfine interactions together with dipolar fields into one single term, and shall often refer to them simply as ‘‘dipolar fields.’’ We define local field \mathbf{H} by

$$\mathbf{H} = \mathbf{H}^0 + \mathbf{H}_d. \quad (3)$$

The third interaction follows from the fact that Mn acetate crystallizes in a tetragonal structure.²⁴ It has been shown that this gives rise to quartic spin terms.²³ In short,

$$\mathcal{H}'_1 = -g\mu_B H_{dz} S_z - A_4 S_z^4, \quad (4)$$

and

$$\mathcal{H}'_2 = -g\mu_B H_x S_x - C(S_+^4 + S_-^4). \quad (5)$$

The stationary Schrödinger equation, $\langle m | \mathcal{H} | \Psi_l \rangle = E_l \langle m | \Psi_l \rangle$ ($|m\rangle$ is defined by $S_z |m\rangle = m |m\rangle$) is easily handled in the form

$$E_m^D \Psi_l(m) + \sum_{m'} u_{m,m'} \Psi_l(m') = E_l \Psi_l(m), \quad (6)$$

where

$$E_m^D = \langle m | \mathcal{H}_0 + \mathcal{H}'_1 | m \rangle, \quad (7)$$

$\Psi_l(m) = \langle m | \Psi_l \rangle$, and

$$u_{m,m'} = \langle m | \mathcal{H}'_2 | m' \rangle. \quad (8)$$

We use index l to number the energy eigenstates of the full Hamiltonian in increasing order of energy. We shall refer to eigenstates and eigenvalues of $\mathcal{H}_0 + \mathcal{H}'_1$ as *unperturbed* states and energies, respectively. Since these states are eigenstates of S_z , we number them with the magnetic quantum number m .

For reasons given in Appendix A, we adopt the values $D \approx 0.69$ K, $H_{dz} \approx H_{dx} \approx 0.06H_1$ ($H_1 \equiv D/g\mu_B$), $C/D \approx 5.7 \times 10^{-5}$, and $A_4/D \approx 5 \times 10^{-4}$ for Mn acetate.

B. Resonance conditions

The unperturbed energies of spin-up (m) and spin-down ($-m-n$) states are equal if $H_z = nH_1$, for $n = 0, \pm 1, \pm 2, \dots$, when $A_4 = 0$. More generally, maximum resonance obtains when

$$H_z = nH_1(1 + \alpha_{mn}), \quad (9)$$

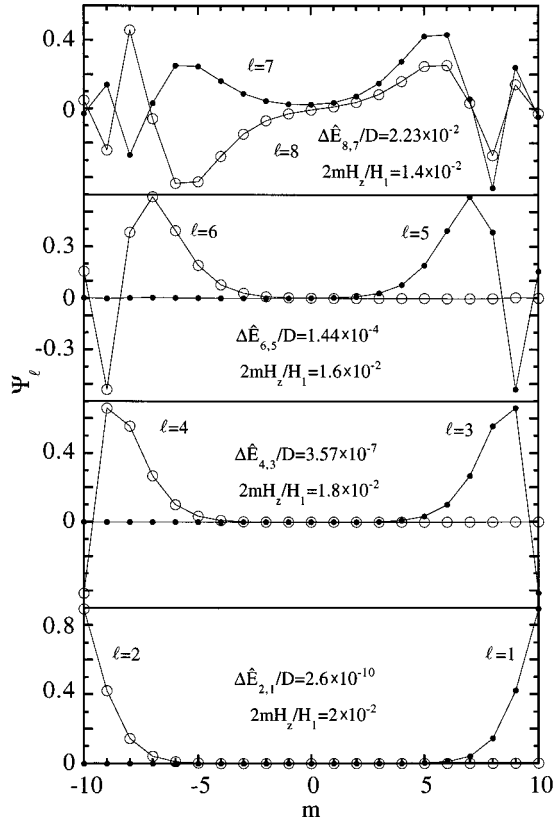


FIG. 1. Wave functions for $C=A_H=0$ and conditions that are not quite resonant, $H_z=10^{-3}H_1$ and $H_x=4H_1$. Straight lines joining \bullet and \circ data points are shown as guides to the eye. Zeeman energies $2H_z m$ and energy splitting values $\Delta \hat{E}_{l+1,l} \equiv E_{l+1} - E_l$ (calculated for $H_z=0$) are given.

where $\alpha_{mn} = (A_4/D)[m^2 + (m+n)^2]$. Since experimental resonances occur at $H_z \approx n0.5$ T in Mn acetate, at least for $n \leq 4$, it follows that $\alpha_{mn} \ll 1$.

Disorder in nuclear and ionic spin orientations contribute random dipolar fields H_{dz} and H_{dx} to \mathcal{H}'_1 and \mathcal{H}'_2 , respectively. Variations in \mathcal{H}'_1 shifts unperturbed energies, and may thus upset resonance conditions, Eq. (9). Let $\Delta \hat{E}_{l+1,l}$ stand for an energy splitting at maximum resonance, that is

$$\Delta \hat{E}_{l+1,l} \equiv \hat{E}_{l+1} - \hat{E}_l, \quad (10)$$

when the two unperturbed states m and $-m-n$ that correspond to $l+1$ and l are degenerate. Increasing strength of \mathcal{H}'_2 widens all energy splittings $\Delta \hat{E}_{l+1,l}$. Let

$$\Delta E_{m,-m-n}^D = |E_m^D - E_{-m-n}^D|. \quad (11)$$

It follows, neglecting α_{mn} , from Eqs. (2), (4), and (7) that

$$\Delta E_{m,-m-n}^D \approx g\mu_B(2m+n)|H_z - nH_1|, \quad (12)$$

which is the Zeeman energy difference between spin-up (m) and spin-down ($-m-n$) unperturbed energy states.

Pairs of states whose energies fulfill $\Delta E_{m,-m-n}^D \gg \Delta \hat{E}_{l+1,l}$ are localized on both sides of the energy barrier (see, for instance, Ref. 1). This is illustrated in Fig. 1. Dividing this inequality by D (recall that $D = g\mu_B H_1$), and substituting Eq. (12) into it, gives

$$\frac{|H_z - nH_1||2m+n|}{H_1} \gg \frac{\Delta \hat{E}_{l+1,l}}{D}. \quad (13)$$

We shall refer to all pairs of states that satisfy Eq. (13) as ‘‘nontunneling’’ or ‘‘tunnel blocked,’’ and to all other states plainly as ‘‘tunneling’’ pairs of states.

C. The joint action of dipolar and crystal fields

Resonant MQT is observed experimentally for $H_z^0 \approx nH_1$ for both even and odd values of n . The dipolar field term, $g\mu_B H_{dx} S_x$, in \mathcal{H}'_2 is necessary for this. Without it, no resonant tunneling would take place since $C(S_+^4 + S_-^4)$ does not couple m and $-(m+n)$ spin states if n is odd [this follows from Schrödinger’s equation and the fact that $u_{m,m'} \propto \delta_{m,m' \pm 4}$, in Eq. (8), if there are no transverse fields]. However, as we argue next, $g\mu_B H_{dx} S_x$ is not sufficient.

Assume now that $C=0$ in \mathcal{H}'_2 . Numerical solution of Schrödinger’s equation [or the lowest-order degenerate perturbation expression, Eq. (B2) in Appendix B] gives (for $H_{dx}=0.06H_1$) $\Delta \hat{E}_{14,13}/D \approx 5 \times 10^{-12}$ for $m=4, -4$ ($l=13, 14$ corresponds to unperturbed energy eigenstates with magnetic quantum numbers $m=4, -4$). Since $H_{dz} \approx H_{dx}$, it follows that the Zeeman energy on the left-hand side of Eq. (13) would be 11 orders of magnitude larger than the right-hand side. Resonant MQT would then be forbidden to proceed through spin states $m=4, -4$ in Mn acetate at $T \sim U/k_B S$ when no external field is applied. This is a serious contradiction with experimental observations.¹⁷ Equally contradictory consequences follow for odd values of n in $H_z \approx nH_1$ [as can be easily checked using Eq. (B2) in Appendix B]. This serious discrepancy with experimental results implies that additional perturbations, such as $C(S_+^4 + S_-^4)$, in Mn acetate must contribute to resonant MQT.

Consider again $H_z=0$, but with $\mathcal{H}'_2 = C(S_+^4 + S_-^4)$ now. Spin states m and $-m$ are then degenerate. Since $u_{m,m'} \propto \delta_{m,m' \pm 4}$ in Eq. (8), this degeneracy is lifted for all even values of m . Numerical solutions of Schrödinger’s equation gives $\Delta \hat{E}_{14,13}/D \approx 0.048$ for $C/D \approx 5.7 \times 10^{-5}$ (given in Appendix A). This number checks against the lowest-order degenerate perturbation result, $\Delta \hat{E}_{14,13}/D \approx 1.5 \times 10^7 (C/D)^2$ which follows from Eq. (B4) for $m=4$, if the given value of C/D is used. The value (0.048) just obtained for $\Delta \hat{E}_{14,13}/D$ is ten orders of magnitude larger than the value of $\Delta \hat{E}_{14,13}/D$ produced by $g\mu_B H_{dx} S_x$ above. This result is encouraging, but does nothing for tunneling when $H_z \approx nH_1$ and n is odd valued.

We are thus forced to consider *both* terms in \mathcal{H}'_2 together. Then, in Eq. (8),

$$u_{m,m'} = a\delta_{m,m' \pm 1} + b\delta_{m,m' \pm 4}, \quad (14)$$

where, $a = (g\mu_B H_{dx}/2)(\langle m|S_+|m'\rangle + \langle m|S_-|m'\rangle)$, and $b = C(\langle m|S_+^4|m'\rangle + \langle m|S_-^4|m'\rangle)$. Clearly, all degeneracies are now lifted. Numerical results for $\Delta \hat{E}_{l+1,l}$ are shown versus l in Fig. 2(a) for $H_z=0$, with $C/D = 5.7 \times 10^{-5}$ and two values of H_{dx} : $10^{-3}H_1$ and $0.06H_1$. Switching on the C term in \mathcal{H}'_2 clearly raises $\Delta \hat{E}_{l+1,l}$ for $l=1, 5, 9 \dots$ by many orders of magnitude in Fig. 2(a), as remarked above. Equally impor-

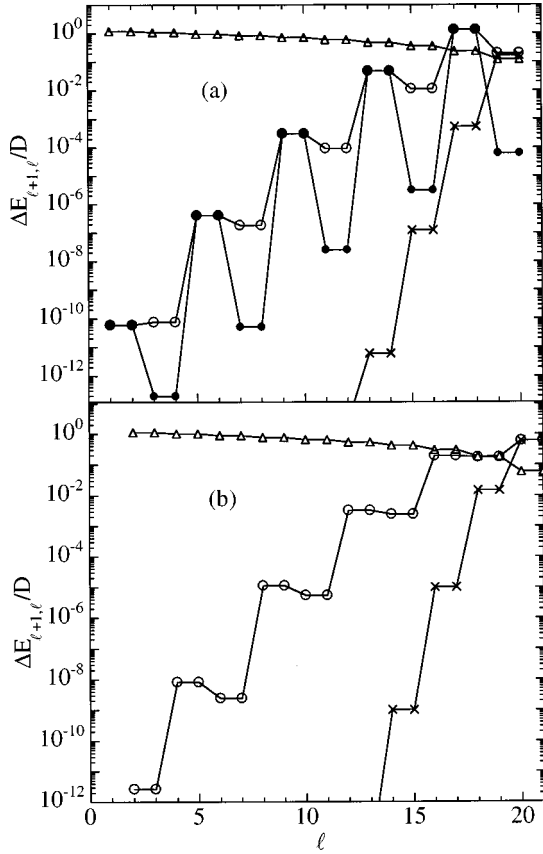


FIG. 2. (a) Energy splitting values $\Delta\hat{E}_{l+1,l}/D$ versus energy-level number l for $H_z=0$. \bullet and \circ stand for $C/D \approx 5.7 \times 10^{-5}$ K, and two values of H_x : $10^{-3}H_1$ and $0.06H_1$, respectively. Data points (\times) for $C=A_4=0$ and $H_x=0.06H_1$ are also shown. \triangle stands for the Zeeman energy blocking term $2mH_{dz}/H_1$, where $H_{dz}=0.06H_1$. Lines are guides to the eye. States $l=15,16$, $l=17,18$, and so on, are superpositions of states $m=4,-4$, $m=3,-3$, etc., respectively, in lowest order degenerate perturbation theory. (b) Same as in (a), but for $H_z \approx H_1$. The value of H_x is important here: $H_x=H_{dx}=0.06H_1$. States $l=14,15$, $l=16,17$, and so on, become states $m=3,-4$, $m=2,-3$, etc., respectively, when $\mathcal{H}'_2 \rightarrow 0$.

tant, switching on the H_x term in \mathcal{H}'_2 raises $\Delta\hat{E}_{l+1,l}$ for $l=3,7,\dots$ from 0 up to the vicinity of the values it takes at other l values. Thus, effective dipolar fields in Mn acetate enable crystal-field interactions to operate at nearly full strength where selection rules would forbid them otherwise. Results for $\Delta\hat{E}_{l+1,l}$ are shown versus l in Fig. 2(b), as in Fig. 2(a), but for $H_z \approx H_1$. Note again that switching on the H_x term raises $\Delta\hat{E}_{l+1,l}$ from 0 up to reasonably high values. In order to be able to estimate which pairs of states tunnel, the Zeeman energy term on the left-hand side of Eq. (13), calculated for $H_z=H_{dz}=0.06H_1$, is also shown in Figs. 2(a) and 2(b). Further insight into the effect by which the joint action of both terms in \mathcal{H}'_2 can raise values of $\Delta\hat{E}_{l+1,l}$ so sharply is given in Appendix B.

Finally, a comment about the interpretation of Fig. 2(a) follows. The Zeeman energy $\Delta E_{4,-4}^D$ shown in Fig. 2(a) was calculated with $H_z=H_{dz}=0.06H_1$. It is approximately ten times larger than $\Delta\hat{E}_{14,13}$. Tunneling through states $m=4,-4$ would be blocked for *all* molecular spins in the

system if the magnetic field were *homogeneous*. However, dipolarlike fields vary randomly over space. It follows that the Zeeman energy of roughly 1 out of 10 spins in the system is *smaller* than $\Delta\hat{E}_{14,13}$, and can therefore tunnel through readily. More quantitative results are given in Sec. IV.

III. RESONANT TUNNELING THROUGH LONG LIVED THERMALLY POPULATED STATES

The purpose of this section is to establish that resonant MQT through thermally activated states in Mn₁₂ acetate takes place incoherently. We show in Sec. III A that the density matrix is approximately diagonal while tunneling takes place and that the process is governed by the master equation. The tunneling process is described in some detail in Sec. III B.

We first check that spin energy eigenstates in Mn acetate are long lived, that is, that

$$\Delta E_{l,l'} \gg \hbar/\tau_0, \quad (15)$$

where τ_0 is a typical lifetime of spin-phonon-induced transitions, and $\Delta E_{l,l'}$ is the energy difference between *any* two energy eigenstates $|E_l\rangle$ and $|E_{l'}\rangle$. Since $\Delta E_{l+1,l}$ is larger than the unperturbed energy $g\mu_B|H_z-nH_1||2m+n|$ (where n is an integer such that $|H_z-nH_1| < H_1$), it suffices to check that

$$g\mu_B|H_z-nH_1||2m+n| \gg \hbar/\tau_0. \quad (16)$$

Substitution of H_{dz} for $|H_z-nH_1|$, and $H_{dz} \approx 0.06H_1 \approx 0.03$ T and $\tau_0 \approx 10^{-7}$ s for Mn acetate, leads (since $|2m+n| \geq 1$) to fulfilment of inequality (16), by approximately three orders of magnitude, and of Eq. (15) *a fortiori*.

Fulfilment of inequality (15) implies that homogeneous line broadening induced by spin-phonon interactions are much smaller than the energy difference between any pair of energy levels (whether they are a tunneling pair or not). This is our basis for applying first-order time-dependent perturbation theory below, as well as for further arguments that lead subsequently to the master equation.

A. Master equation

Consider a spin that is initially in state $|E_i\rangle$, and let $U(t)$ be the time evolution transformation for the system that is made up of the spin of interest and the heat bath. Then, the reduced density matrix at time t is given by

$$\begin{aligned} \langle E_l|\rho(t)|E_{l'}\rangle &= \sum_{r,r'} P_r \langle \mathcal{E}_{r'}|\langle E_l|U(t)|E_i\rangle|\mathcal{E}_r\rangle \\ &\quad \times \langle \mathcal{E}_r|\langle E_i|U^\dagger(t)|E_{l'}\rangle|\mathcal{E}_{r'}\rangle, \end{aligned} \quad (17)$$

where $|\mathcal{E}_r\rangle$ is an energy eigenstate of the heat bath, and P_r is the corresponding thermal probability. Assume the interaction between the spin of interest and a heat bath is weak (as shown above to be the case for Mn acetate), and that the heat bath is in thermal equilibrium. It follows from first-order time-dependent perturbation theory²⁵ [in the interaction representation, in which the Hamiltonian in $U(t)$ is just some spin-phonon interaction in this case] that each transition *amplitude* in Eq. (17) ceases growing with time when t

$\geq \hbar/\Delta\tilde{E}$, where $\Delta\tilde{E}$ is the corresponding difference between the initial and final energies of the spin plus heat bath system. Note that the initial energies of both heat bath and spin system are the same for both probability amplitudes in Eq. (17), but whereas the two final energies of the spin system are different, the two final energies of the heat bath are not. [When, for instance, $\Delta\tilde{E}=0$ for one of the two amplitudes in the sum in Eq. (17), then $\Delta\tilde{E}=\pm(E_l-E_{l'})$ for the other amplitude.] Taking this into account, it is not too difficult to see that

$$\langle E_l|\rho(t)|E_{l'}\rangle/\langle E_l|\rho(t)|E_l\rangle \approx 0 \quad (18)$$

for $t \gg \hbar/|E_l-E_{l'}|$. In short, $\langle E_{l'}|\rho(t)|E_l\rangle$ becomes approximately diagonal most of the time (since we assume that all states $|E_l\rangle$ are long lived, that is, that $\tau_0 \gg \hbar/|E_l-E_{l'}|$, as in Mn acetate). Defining, $P_l(t) \equiv \langle E_l|\rho(t)|E_l\rangle$, we may therefore write the desired equation,

$$\frac{dP_l}{dt} = \sum_{l'} (w_{l \leftarrow l'} P_{l'} - w_{l' \leftarrow l} P_l), \quad (19)$$

where $w_{l \leftarrow l'}$ follows from Fermi's golden rule, using the appropriate spin-phonon interaction. Hartmann-Boutroun *et al.* (Ref. 23) have obtained

$$w_{l' \leftarrow l} = q |E_l - E_{l'}|^3 |\langle E_{l'}|B(\mathbf{S})|E_l\rangle|^2 A_{l,l'}, \quad (20)$$

where $A_{l,l'} = n_{l,l'}$ and $A_{l,l'} = (1 + n_{l,l'})$ for upward and downward, respectively, in energy transitions, $n_{l,l'}$ is the number of available thermal phonons for an $\Delta E_{l',l} = E_{l'} - E_l \geq 0$ transition, that is, $n_{l,l'} = 1/[\exp(\Delta E_{l',l}/k_B T) - 1]$, q is defined in Ref. 23 [but we determine it for Mn acetate by fitting the Arrhenius behavior we obtain for Γ to the experimental one, $\tau_0^{-1} \exp(-U/k_B T)$, with $\tau_0 \approx 10^{-7}$ s (Ref. 17)], and $B(\mathbf{S})$ is a spin operator. We use the simplest time-reversal invariant Hermitian expression $S_x S_z + S_z S_x$ for it. The value of q obtained is approximately halfway between the bounds that were obtained by Villain *et al.*²⁶

Some care must be taken in the application of Eq. (19). It has been assumed that, as in Mn acetate, inequality (16) holds. Care must therefore be taken that it is not inadvertently violated when applying the master equation. This may be prevented from happening by not allowing H_z to come within a distance $\hbar/(\tau_0 g \mu_B)$ from the resonant values of H_z . Failure to do something to this effect for low-lying energy states for which $\Delta\hat{E}_{l+1,l} \gg \hbar/\tau_0$ is not fulfilled leads to error. Resonant tunneling would be allowed when it should not be. This scheme is valid as long as shifts in H_z in the laboratory by this amount are innocuous. For Mn acetate $\tau_0 \sim 10^{-7}$ s,¹⁷ therefore $\hbar/(\tau_0 g \mu_B)$ is roughly three orders of magnitude smaller than H_{dz} . In our calculations, we have not allowed H_z to come within $10^{-3} H_1$ (that is, $\frac{1}{60}$ of the value we have adopted for H_{dz}) of any of its resonance values. Before we turn our attention, in Sec. IV, to quantitative results obtained with the master equation, we briefly describe how resonant tunneling through thermally populated states takes place in Mn acetate.

B. Description of thermally activated resonant tunneling

Let us assume some temperature *not* much smaller than $U/k_B S$. Let $H_x = 4H_1$, $H_z = 10^{-3} H_1$, and $C = A_4 = 0$ for which some energy eigenstates are shown in Fig. 1. Suppose the system is initially in some spin-down low-lying energy state, the $l=6$ state, say. Now, in first-order transitions, spin-phonon interactions give $m \rightarrow m \pm 1$. Therefore, transitions between wave functions on opposite sides of the anisotropy barrier in Fig. 1 are very weak for all $l < 7$. Spin-phonon interactions can generate, out of state $l=6$, a wave function ϕ , with an initially ill-defined energy, that is a superposition of $l=7$ and $l=8$ states. Initially, $\langle \phi|S_z|\phi\rangle < 0$ and $\langle E_{l=7}|\rho|E_{l=8}\rangle \neq 0$ since $\rho = |\phi\rangle\langle\phi|$ then. However, it was shown above that $\langle E_{l=7}|\rho(t)|E_{l=8}\rangle$ vanishes after a time of about $\hbar/\Delta E_{8,7}$. If, as we assume, $\tau_0 \gg \hbar/\Delta E_{8,7}$, then the system remains in this incoherent superposition of states, $l=7$ and $l=8$, most of the time τ_0 . A down in energy transition to a spin-up state $l=5$ (and from there on down to state $l=1$, subsequently) can therefore occur from either state $l=7$ or state $l=8$.

A semiquantitative account follows. Let $\Psi_{l=7} \propto (\psi_{\text{right}} + \epsilon \psi_{\text{left}})$ and $\Psi_{l=8} \propto (\epsilon \psi_{\text{right}} - \psi_{\text{left}})$, where ψ_{left} and ψ_{right} are approximately localized on the left and right side, respectively, of the barrier. [States Ψ_l are depicted in Fig. (1)]. It follows straightforwardly that the rate γ for a transition from the spin-down state $\Psi_{l=6}$ to the spin-up state $\Psi_{l=5}$, through the 7,8 pair of states, is given by

$$\gamma \propto \mathcal{R}_{5 \leftarrow 7} \mathcal{R}_{7 \leftarrow 6} + \mathcal{R}_{5 \leftarrow 8} \mathcal{R}_{8 \leftarrow 6}, \quad (21)$$

where

$$\mathcal{R}_{l \leftarrow l'} \equiv |\langle \Psi_l | B(\mathbf{S}) | \Psi_{l'} \rangle|^2, \quad (22)$$

since we have established that there are no interference effects (it follows from the master equation that *probabilities*, not probability *amplitudes*, are to be added). For any reasonable operator $B(\mathbf{S})$ (such as $S_x S_z + S_z S_x$) that does not shift the value of S_z by too many units upon acting once, it follows that

$$\gamma \sim \epsilon^2 / (1 + \epsilon^2)^2. \quad (23)$$

The main features of the observed resonant tunneling effects in Mn acetate follow from the fact that $\epsilon = 1$ for $H_z = 0$, but $\epsilon \approx 0$ for $g \mu_B H_z m \gg \Delta\hat{E}_{l+1,l}$.

Additional effects have to be taken into account in order to obtain tunneling rates that can be compared with experiment. The actual transition probabilities $w_{l \leftarrow l'}$ have to be evaluated in order to obtain temperature dependences and proportionality constants. In addition, higher-energy pairs of states with small non-negligible thermal populations contribute some to spin tunneling rates. That is all, of course, taken care of when the master equation is applied. Finally, the spin-relaxation rate obtained $\Gamma(H_z)$ has to be convoluted with a distribution of random dipolar fields (that give inhomogeneous broadening). All of this is done in the next section.

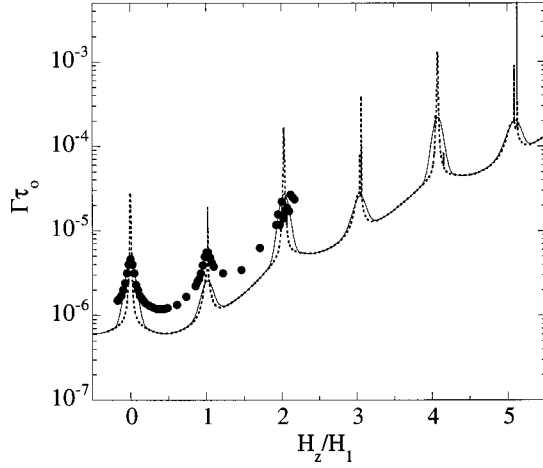


FIG. 3. Data points for the spin-relaxation rate versus H_z/H_1 for $T=5$ K. Full and dashed lines stand for $\Gamma_b\tau_0$ and $\Gamma_u\tau_0$, respectively. [Γ_u is defined in the text as the *unbroadened* relaxation rate, that is, it does not include (Γ_b does) the inhomogeneous broadening that is produced by the z component or random magnetic dipolar fields]. Experimental data points (●) are also shown for comparison. The experimental points were taken from Refs. 15,17.

IV. COMPARISON WITH EXPERIMENTS IN Mn_{12} ACETATE

In this section, we report results we have obtained through numerical application of the master equation, Eq. (19). These results can be compared to data from recent observations of resonant MQT in Mn acetate crystals. In analogy with experiment, the system is assumed to be in equilibrium at some temperature T , and magnetic field \mathbf{H} , for $t < 0$. At $t = 0$, $H_z \rightarrow H_z + 10^{-3}H_1$, is suddenly applied along the anisotropy axis. We study the ensuing time evolution of $\langle S_z \rangle_t$ [that we shall refer to as $m(t)$]. We have always found that $m(t)$ relaxes to its equilibrium value $\langle m \rangle$ exponentially, after a brief nonexponential relaxation. We are interested in the relaxation rate Γ , defined by the long-time behavior $\delta m(t) \propto \exp(-\Gamma t)$, as a function of H_z , H_x , and T .

For reasons given above, we obtain Γ for values $H_z \geq 10^{-3}H_1$ and $H_x \geq H_{dx} = 0.06H_1$. Thus, if no external field is applied we put $H_z = 10^{-3}H_1$ and $H_x = H_{dx} = 0.06H_1$. We also take into account broadening effects produced by inhomogeneous effective longitudinal dipolar fields. To this end, we assume a Gaussian distribution $\mathcal{P}(H''_{dz})$ of dipolar field H''_{dz} , with a half width at half maximum of $0.06H_1$. A broadened relaxation rate, given by $\Gamma_b(H'_z) = \int \mathcal{P}(H'_z - H_z) \Gamma(H'_z) dH'_z$, follows. For clarity's sake, we let Γ_u stand for Γ (the unbroadened one). In addition, all results quoted below are obtained using the values of D , A_4/D , C/D , and τ_0 given in Appendix A.

$\Gamma_b\tau_0$ and $\Gamma_u\tau_0$ versus H_z/H_1 are shown in Fig. 3 for $T = 5$ K. There is reasonable agreement with experiment.^{15,17} Some satellites show for $\Gamma_u\tau_0$ for $n \geq 4$. For lower values of n , resonances that correspond to tunneling through different levels pile up at nearly the same values of H_z .

Magnetization m hysteresis curves follow straightforwardly from knowledge of $\Gamma_b(H_z^0)$. We vary H_z^0 in the range $-6H_1 < H_z^0 < 6H_1$ in steps of $10^{-2}H_1$. H_z^0 is kept constant at each value of H_z^0 , for $5.7 \times 10^8 \tau_0$ s [τ_0 has been determined

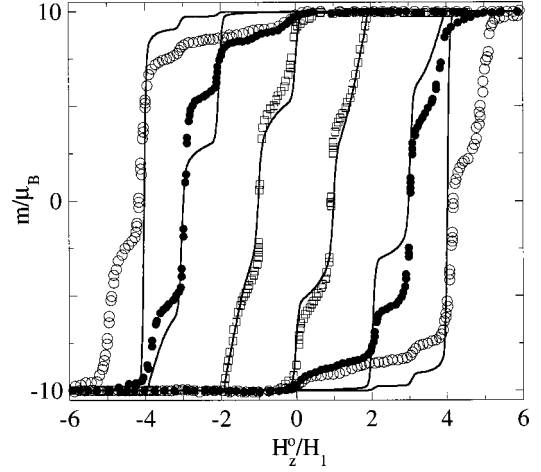


FIG. 4. Magnetization, in Bohr magneton units, versus H_z^0/H_1 for various temperatures. □, ●, and ○ stand for $T=2.64$, 2.10, and 1.77 K, respectively. The schedule that specifies how H_z^0 varies with time is given in the text. The continuous line stands for our numerical results. The experimental points were taken from the paper by Thomas *et al.* in Ref. 16.

experimentally to lie in the range $6 \times 10^{-8} \text{ s} \leq \tau_0 \leq 2 \times 10^{-7} \text{ s}$ (Refs. 15,17)]. Our steps are about five times smaller than the ones that were taken experimentally, but the over all sweeping rate is between $8.6 \times 10^{-5} H_1/\text{s}$ and $3 \times 10^{-4} H_1/\text{s}$, which is to be compared with an experimental rate of $8.3 \times 10^{-5} H_1/\text{s}$.¹⁶ The curves obtained, exhibited in Fig. 4, reproduce the main features of the hysteresis curves that are observed experimentally.

The activation energy U_{eff} , obtained from Arrhenius' plots in the temperature range $3 \leq k_B T/D \leq 10$, is plotted in Fig. 5 versus H_z^0 . Experimental data points are also shown for comparison. No transverse field is applied. The classical (no tunneling) activation energy barrier U_{cl} is also shown. The level through which resonant MQT proceeds can be found from the data exhibited in this figure. For instance, for $H_z^0 = 0$, $U_{\text{cl}}/D \approx 105$ and $U_{\text{eff}}/D \approx 89$, when $16 \approx S^2 - m^2$

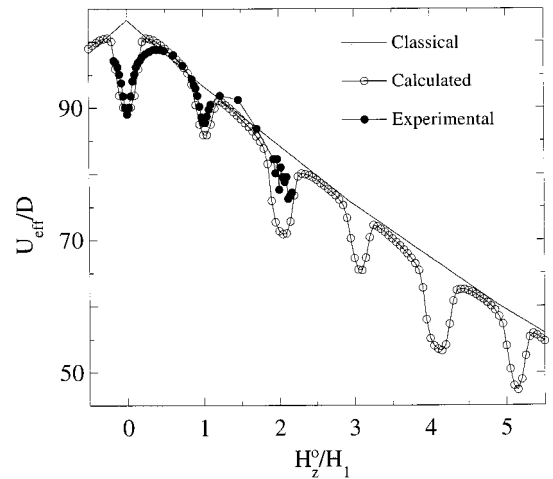


FIG. 5. Activation energy U_{eff}/D (in the temperature range $0.3 \leq k_B T/D \leq 10$) versus H_z^0 . Experimental data points are also shown for comparison. No transverse field is applied. The classical energy barrier $U_{\text{cl}} = DS^2 + A_4 S^4 - g \mu_B H_z^0 S$ is also shown (as a continuous line). The experimental points were taken from Ref. 17.

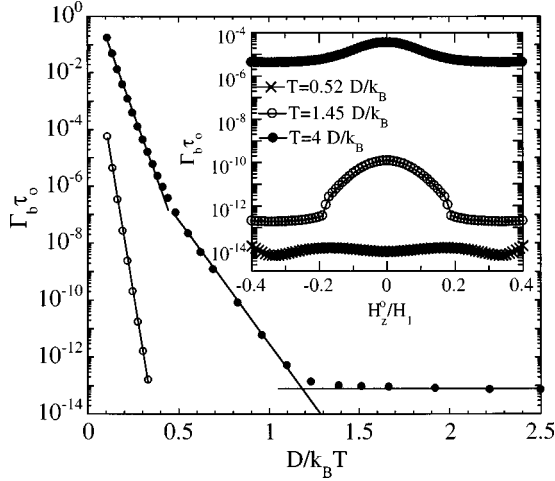


FIG. 6. Data points for $\Gamma_b \tau_0$ versus $D/k_B T$. \circ and \bullet stand for $H_x = 0.06 H_1$ (i.e., the dipolar field value), and for $H_x = 5.5 H_1$, respectively. Γ_b versus H_z^0 is shown in the inset for three different temperatures.

+ $(A_4/D)(S^4 - m^4)$, and $m \approx \pm 4$ follows, in accordance with experiments.¹⁷

We next predict behavior of Γ as a function of an applied transverse field, which may be compared with future experiments. Results for $\Gamma_b \tau_0$ versus $D/k_B T$ are given in Fig. 6. The curve for no applied external field shows that, in the temperature range shown, tunneling takes place through one level (since a straight line fits the data well). Its energy above the ground state, $U_{\text{eff}}/D \approx 89$, follows from the slope of the curve. (We have chosen the value $D \approx 0.69$ K, in Appendix B, in order to obtain agreement with the experimentally measured $U_{\text{eff}} \approx 61$ K, after $A_4/D \approx 5 \times 10^{-5}$ was adopted.) The results shown in Fig. 6 for a transverse field $H_x = 5.5 H_1$ exhibit three different regimes. The nearly horizontal piece is for tunneling through the ground state. As the temperature rises, tunneling shifts to upper levels. The other two pieces for $D/k_B T \lesssim 1.1$ correspond to tunneling through the first and second excited states. Γ_b versus H_z^0 is shown in the inset for three different temperatures. It follows from it that while tunneling through both excited states is resonant, it is not so for the ground state near $H_z^0 = 0$. Tunneling through the ground state must therefore be nonresonant for smaller values of H_x . (We however find resonances for other resonant values of H_z , that is, when $H_z^0 \approx n H_1$, and $n \geq 1$, for $H_x = 5.5 H_1$.)

The spin-relaxation rate versus transverse field, is shown in Fig. 7 for the zeroth and first resonances, that is, for $H_z \approx 0$ and $H_z \approx H_1$. Resonant tunneling becomes blocked for $H_z \approx H_1$ as $H_x \rightarrow 0$, and consequently the two shown curves differ significantly there. They are not significantly different elsewhere. The portion of the $H_z \approx H_1$ curve for $H_x/H_1 \lesssim 0.06$ is experimentally unobservable, because of dipolar fields. When $H_x/H_1 \gtrsim 10$ the ground-state tunneling pair becomes unblocked, and unassisted tunneling can then take place, but this is beyond the scope of the present contribution.

V. CONCLUSIONS

Summing up, we have found the mechanism that generates energy splittings that are large enough to account for the

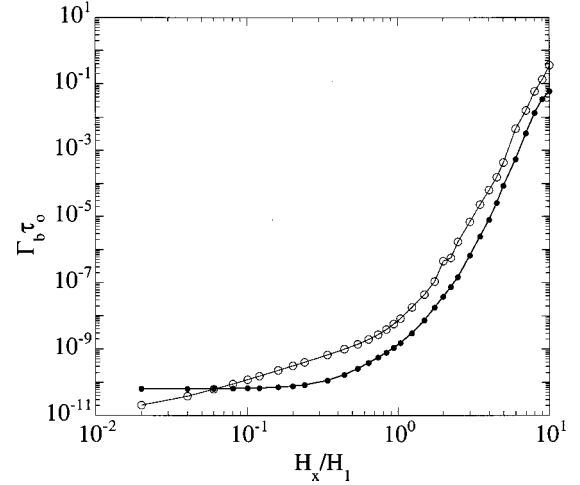


FIG. 7. The spin-relaxation rate $\Gamma_b \tau_0$ versus transverse field, in units of H_1 , for the \bullet zeroth and \circ first resonances, that is, for $H_z^0 = 0$ and $H_z^0 \approx H_1$. Resonant tunneling becomes blocked for $H_z^0 \approx H_1$ as $H_x \rightarrow 0$, and consequently the two shown curves differ significantly there. The portion of the $H_z^0 \approx H_1$ curve for $H_x/H_1 \lesssim 0.06$ is experimentally unobservable, because of dipolar fields.

resonant MQT through thermally populated states that has been observed experimentally in Mn acetate.¹⁴⁻¹⁷ It is a combination of large random transverse fields (that may originate in hyperfine interactions) and crystal-field effects proposed in Refs. 21,23. We have also explained how resonant MQT through thermally excited states takes place, even though decoherence effects do not allow spins to oscillate between up and down states. We have applied a master equation, under the conditions we have established for its validity, to obtain spin-relaxation rates that follow from resonant MQT through thermally populated states in Mn acetate. The framework we propose for MQT applies equally well to other MQT systems if, as in Mn acetate, $\hbar/\tau_0 \ll g \mu_B H_d S$ is fulfilled.

ACKNOWLEDGMENTS

We are grateful to Professor Pablo Alonso for enlightening remarks. We have profited from a discussion with Professor E. Chudnovsky, Professor A. Leggett, and Professor J. Tejada. We thank Professor J. Villain for results of Ref. 23. F.L. is grateful to Dr. J. Chaboy for making available a workstation for some numerical work. F.L. and J.B. acknowledge partial financial support from CICYT through Grant No. MAT96/448, and J.F. is grateful for DGES Grant No. PB95-0797 (all from the government of Spain).

APPENDIX A

Here we explain how we arrive at the values $D \approx 0.69$ K, $C/D \approx 5.7 \times 10^{-5}$, and $A_4/D \approx 5 \times 10^{-4}$. No satellites are seen experimentally in any of the resonances at $H_z^0 \approx n H_1$ that are observed experimentally for $n \leq 4$. We also know that tunneling takes place through $m = 4, -4$ spin states for $H_z^0 = 0$.¹⁷ We expect tunneling to take place, for other resonant values of H_z^0 , through pairs of states whose energy lies approximately as far below the barrier top as the tunneling states for $H_z^0 = 0$ do. Taking this into account, making use of

Eq. (9), leads to the bound $|A_4/D| \leq 5 \times 10^{-4}$.

The activation energy U_{eff} for tunneling, for $H_z^0 = 0$, through the $m = 4, -4$ spin states, has been experimentally determined¹⁷ to be $U_{\text{eff}} \approx 61$ K. It follows from Eqs. (2) and (4) that $U_{\text{eff}} \approx 84D + 9744A_4$.

Making use of the master equation we obtain U_{eff} versus $1/T$. In order to obtain agreement with Arrhenius plots that follow from experiments we have to put $C/D \sim 5 \times 10^{-5}$. The precise value of C/D depends on the value of A_4 . But now we know that $|A_4/C| \leq 10$. On the other hand, $A_4/C = 70$ for cubic crystals²³ (but note that Mn acetate crystallizes on a tetragonal structure). On this basis we adopt the upper bound we have for A_4 , that is, we set $A_4/D \approx 5 \times 10^{-4}$. We thus have $A_4/C \sim 10$. Having fixed the value of A_4 , we obtain the best fit to experimental data with $C/D = 5.7 \times 10^{-5}$. From these fits, we estimate C/D to be in the range $2 \times 10^{-5} \leq C/D \leq 10^{-4}$, which overlaps with the range given for it in Ref. 23. The value $D \approx 0.69$ K follows from $U_{\text{eff}} \approx 84D + 9744A_4$ and from the value of A_4 just determined. These values give 14.3 K for the energy difference between the ground state and the first excited state. This is in good agreement with the value of 14.4 K determined from electron paramagnetic resonance.¹²

APPENDIX B

Lowest-order degenerate perturbation expressions for the energy splitting of degenerate states m and m' follow from Ref. 27,

$$\Delta \hat{E}_{l+1,l} = 2 \left\langle m \left| \mathcal{H}'_2 \frac{1}{\mathcal{H}_D - E_m^D} \mathcal{H}'_2 \frac{1}{\mathcal{H}_D - E_m^D} \dots \mathcal{H}'_2 \right| m' \right\rangle, \quad (\text{B1})$$

where $\mathcal{H}_D = \mathcal{H}_0 + \mathcal{H}'_1$, and index l numbers the perturbed energy eigenstates in increasing order of energy, and m is the magnetic quantum number of the unperturbed states. States m and m' are degenerate if $H_z \approx nH_1$. Consider first $\mathcal{H}'_2 = -g\mu_B H_x S_x$. Since $m' = -m - n$, and $S_x \propto (S_+ + S_-)$, it follows that \mathcal{H}'_2 must act $2m + n$ times in Eq. (B1). It follows, using $\langle m' + 1 | S_+ | m' \rangle = [(S - m')(S + m' + 1)]^{1/2}$, that

$$\Delta \hat{E}_{l+1,l} = f(m, n) \left[\frac{H_x}{2H_1 S} \right]^{2(m+n/2)}, \quad (\text{B2})$$

where

$$f(m, n) = \frac{2DS^{2(m+n/2)}}{[(2m+n-1)!]^2} \sqrt{\frac{(S+m+n)!(S+m)!}{(S-m-n)!(S-m)!}}. \quad (\text{B3})$$

This is an extension to nonzero integer values of n of Garanin's perturbation results.²⁷ [Equation (B2) appears also in recent results of Garanin and Chudnovsky.]

Another case of interest to us is $\mathcal{H}'_2 = C(S_+^4 + S_-^4)$. It follows from Eq. (B1) that $\Delta \hat{E}_{l+1,l} = 0$ for $H_z \approx nH_1$ and n odd. We give the result only for $n = 0$. It follows then from Eq. (B1) that

$$\Delta \hat{E}_{l+1,l}/D = 32 \left(\frac{C}{16D} \right)^{m/2} \frac{1}{(m/2-1)!^2} \frac{(S+m)!}{(S-m)!} \quad (\text{B4})$$

for even m , and $\Delta \hat{E}_{l+1,l}/D = 0$ for odd m .

A hint for why values of $\Delta \hat{E}$ are raised so sharply by the joint action of both terms in \mathcal{H}'_2 follows. Consider $H_z \approx nH_1$ for odd n . Let, for the sake of definiteness, $n = 1$ and m even. Then, $m' = -m - 1$. In all leading terms, $C(S_+^4 + S_-^4)$ would appear $m/2$ times for \mathcal{H}'_2 in Eq. (B1), and $g\mu_B H_x S_x$ would replace \mathcal{H}'_2 once. There are $m/2 + 1$ such terms, one for each position of the $g\mu_B H_x S_x$ term in Eq. (B1).

Finally, we discuss why approximation of hyperfine interactions by dipolar magnetic fields for resonant MQT of Mn acetate makes sense, at least if $2m + n$ is a multiple of 4 (such as for tunneling through $m = 4, -4$ states that takes place for $H_z = 0$). We split the hyperfine interaction of an electron spin \mathbf{S} with a nuclear spin \mathbf{I} into parts $A_z S_z I_z$ and $A_x S_x I_x + A_y S_y I_y$ which we group with terms in \mathcal{H}'_2 and \mathcal{H}'_1 , respectively. States $|m\rangle$ and $|m'\rangle$ in Eq. (B1) should now be replaced by $|m, \{M\}\rangle$ and $|m', \{M'\}\rangle$, where $\{M\}$ and $\{M'\}$ are sets of z -component nuclear-spin quantum numbers. If $2m + n$ is a multiple of 4, a good approximation to $\Delta \hat{E}_{l+1,l}$ is obtained by replacing every \mathcal{H}'_2 in Eq. (B1) by $C(S_+^4 + S_-^4)$. It follows then that sets $\{M\}$ and $\{M'\}$ are equal, and that hyperfine interactions do not contribute to $\Delta \hat{E}_{l+1,l}$. They do contribute to $\Delta E_{m, -m-n}^D$ through \mathcal{H}'_1 , but, for each nuclear spin, I_z is to be replaced by a c number (since sets $\{M\}$ and $\{M'\}$ are equal) that depends on $\{M\}$. Furthermore, since $A_x \approx A_y \approx A_z$,²³ we replace hyperfine interactions by isotropically distributed magnetic dipolar fields. For $H_z \approx nH_1$ and n odd the above argument does not go through. Further consideration of this point is beyond the scope of this paper. In order to make progress, we nevertheless approximate hyperfine interactions by dipolar fields for all H_z .

*Author to whom correspondence should be addressed: julioF@posta.unizar.es Postal address: ICMA, Facultad de Ciencias, E-50009 Zaragoza, Spain.

¹A. J. Leggett, S. Chakravarty, A. T. Dorsey, M. P. A. Fisher, A. Garg, and W. Zwerger, Rev. Mod. Phys. **59**, 1 (1987).

²See, for instance, P. C. E. Stamp, Nature (London) **383**, 125 (1996); E. M. Chudnovsky, Science **274**, 938 (1996); B. Schwarzschild, Phys. Today **50** (1), 17 (1997).

³E. H. Frei, S. Shtrikman, and D. Treves, Phys. Rev. **106**, 446 (1957).

⁴L. Néel, Ann. Geophys. (C.N.R.S.) **5**, 99 (1949).

⁵J. L. van Hemmen and A. Süto, Europhys. Lett. **1**, 481 (1986); M.

Enz and R. Schilling, J. Phys. C **19**, 1765 (1986); E. M. Chudnovsky and L. Gunther, Phys. Rev. Lett. **60**, 661 (1988); Phys. Rev. B **37**, 9455 (1988); A. Garg and G. H. Kim, *ibid.* **45**, 12 921 (1992); M. C. Miguel and E. M. Chudnovsky, *ibid.* **54**, 388 (1996).

⁶E. M. Chudnovsky, J. Magn. Magn. Mater. **140-144**, 1821 (1995).

⁷Ll. Balcells, J. L. Tholence, S. Linderth, B. Barbara, and J. Tejada, Z. Phys. B **89**, 209 (1992); J. Tejada, Ll. Balcells, S. Linderth, R. Perzynski, B. Rigau, B. Barbara, and J. C. Bacri, J. Appl. Phys. **73**, 6952 (1993); B. Barbara, L. C. Sampaio, J. E. Wegrowe, B. A. Ratnam, A. Marchand, C. Paulsen, M. A. Novak, J. L. Tholence, M. Uehara, and D. Fruchart, *ibid.* **73**, 6703

- (1993); J. Tejada and X. X. Zhang, *J. Phys. C* **6**, 263 (1994); X. X. Zhang and J. Tejada, *J. Magn. Magn. Mater.* **129**, L109 (1994); X. X. Zhang, J. M. Hernández, J. Tejada, and R. Ziolo, *Phys. Rev. B* **54**, 4101 (1996).
- ⁸D. D. Awschalom, M. A. McCord, and G. Grinstein, *Phys. Rev. Lett.* **65**, 783 (1990); D. D. Awschalom, J. F. Smyth, G. Grinstein, D. P. DiVincenzo, and D. Loss, *ibid.* **68**, 3092 (1992).
- ⁹For arguments that coherent magnetic quantum tunneling has indeed been observed in systems studied in Ref. 8, see, for instance, D. D. Awschalom, D. P. DiVincenzo, G. Grinstein, and D. Loss, *Phys. Rev. Lett.* **71**, 4276 (1993); S. Gider and D. D. Awschalom, *Science* **268**, 77 (1995); S. Gider, D. D. Awschalom, D. P. DiVincenzo, and D. Loss, *ibid.* **272**, 425 (1996).
- ¹⁰For skeptical views about the evidence that coherent magnetic quantum tunneling has been observed in systems studied in Ref. 8, see, for instance, A. Garg, *Phys. Rev. Lett.* **70**, 2198 (1993); **71**, 4249 (1993); **74**, 1458 (1995); J. Tejada, *Science* **272**, 424 (1996); A. Garg, *ibid.* **272**, 424 (1996).
- ¹¹See, for instance, B. Barbara and L. Gunther, *J. Magn. Magn. Mater.* **128**, 35 (1993).
- ¹²A. Caneschi, D. Gatteschi, and R. Sessoli, *J. Am. Chem. Soc.* **113**, 5873 (1991); D. Gatteschi, *Science* **265**, 1054 (1994).
- ¹³R. Sessoli, D. Gatteschi, A. Caneschi, and M. A. Novak, *Nature (London)* **365**, 141 (1993).
- ¹⁴J. R. Friedman, M. P. Sarachik, J. Tejada, and R. Ziolo, *Phys. Rev. Lett.* **76**, 3830 (1996).
- ¹⁵J. M. Hernández, X. X. Zhang, F. Luis, J. Bartolomé, J. Tejada, and R. Ziolo, *Europhys. Lett.* **35**, 301 (1996).
- ¹⁶L. Thomas, F. Lioni, R. Ballou, D. Gatteschi, R. Sessoli, and B. Barbara, *Nature (London)* **383**, 145 (1996); J. M. Hernández, X. X. Zhang, F. Luis, J. Tejada, J. R. Friedman, M. Sarachik, and R. Ziolo, *Phys. Rev. B* **55**, 5858 (1997).
- ¹⁷F. Luis, J. Bartolomé, J. F. Fernández, J. Tejada, J. M. Hernández, X. X. Zhang, and R. Ziolo, *Phys. Rev. B* **55**, 11 448 (1997).
- ¹⁸We speak of “resonance” if an *isolated* spin can oscillate periodically between up and down states, even if it cannot be observed to do so because interactions with a heat bath decohere the two resonant states under experimental conditions.
- ¹⁹See, for instance, P.C.E. Stamp, *Nature (London)* **383**, 125 (1996).
- ²⁰C. Paulsen, J. G. Park, B. Barbara, R. Sessoli, and A. Caneschi, *J. Magn. Magn. Mater.* **140-144**, 379 (1995).
- ²¹P. Politi, A. Rettori, F. Hartmann-Boutron, and J. Villain, *Phys. Rev. Lett.* **75**, 537 (1996); **76**, 3041 (1996); A. L. Burin, N. V. Prokof'ev, and P. C. E. Stamp, *ibid.* **76**, 3040 (1996).
- ²²For additional comments about questions that remain unanswered, see P. Politi, A. Rettori, F. Hartmann-Boutron, and J. Villain, *Phys. Rev. Lett.* **76**, 3040 (1996); A. L. Burin, N. V. Prokof'ev, and P. C. E. Stamp, *ibid.* **76**, 3041 (1996).
- ²³F. Hartmann-Boutron, P. Politi, and J. Villain, *Int. J. Mod. Phys. B* **10**, 2577 (1996).
- ²⁴T. Lis, *Acta Crystallogr., Sect. B Chem.* **36**, 2042 (1980).
- ²⁵See, for instance, A. S. Davydov, *Quantum Mechanics* (Addison-Wesley, Oxford, 1965), p. 294.
- ²⁶J. Villain, F. Hartmann-Boutron, R. Sessoli, and A. Rettori, *Europhys. Lett.* **27**, 159 (1994).
- ²⁷D. A. Garanin, *J. Phys. A* **24**, L61 (1991); D. A. Garanin and E. M. Chudnovsky, *Phys. Rev. B* **56**, 11 102 (1997).